ACADÉMIE
DES SCIENCES
INSTITUT DE FRANCE

Comptes Rendus

Géoscience

Sciences de la Planète

Abel Guihou, Baptiste Suchéras-Marx, Thierry Tortosa, Pierre Deschamps and Yves Dutour

Possibilities, challenges, and limitations of dinosaur eggshells LA-ICP-MS U–Pb dating based on samples from Provence (Upper Cretaceous, France)

Volume 358 (2026), p. 353-368

Online since: 11 June 2026

https://doi.org/10.5802/crgeos.338

The Comptes Rendus. Géoscience — Sciences de la Planète *are a member of the Mersenne Center for open scientific publishing*
www.centre-mersenne.org — e-ISSN : 1778-7025

ACADÉMIE DES SCIENCES
INSTITUT DE FRANCE

Comptes Rendus. Géoscience — Sciences de la Planète
2026, Vol. 358, p. 353-368
https://doi.org/10.5802/crgeos.338

Research article
Sedimentology, stratigraphy, basin geology

Possibilities, challenges, and limitations of dinosaur eggshells LA-ICP-MS U–Pb dating based on samples from Provence (Upper Cretaceous, France)

Abel Guihou [*,#,a], **Baptiste Suchéras-Marx** [*,#,a], **Thierry Tortosa** [b], **Pierre Deschamps** [a] **and Yves Dutour** [c]

[a] Aix Marseille Univ, CNRS, IRD, INRAE, CEREGE, Aix-en-Provence, France

[b] Réserve Naturelle de Sainte-Victoire, DEGPR, Département des Bouches-du-Rhône, Marseille, France

[c] Museum of Natural History of Aix-en-Provence, France

E-mails: guihou@cerege.fr (A. Guihou), sucheras-marx@cerege.fr (B. Suchéras-Marx)

Abstract. Obtaining accurate chronostratigraphic constraints on continental deposits is challenging, necessitating innovative dating approaches. Here, we investigate the feasibility of Laser Ablation Inductively Coupled Plasma Mass Spectrometry (LA-ICP-MS) U–Pb dating of dinosaur eggshell fragments from the Late Cretaceous of Provence, France. Preliminary optical, Scanning Electron Microscopy (SEM), and cathodoluminescence (CL) analyses were critical for identifying zones of optimal preservation and mitigating potential diagenetic contamination. Results from two samples attributed to *Megaloolithus mamillare* and *Cairanoolithus dughii* yielded ages of 67.4 ± 4.4 Ma (2s, $n = 60$) and 69.5 ± 9.9 (2s, $n = 50$), respectively, broadly consistent with regional stratigraphic markers. Element mapping reveals significant spatial variation in U and Pb concentrations within individual eggshells, with zones of high contamination contrasting with well-preserved cores. The data highlight the crucial role of diagenesis and organic matter in influencing U–Pb system behavior, although it appears to be limited to early diagenesis. While LA-ICP-MS U–Pb dating of dinosaur eggshells presents substantial challenges, this study demonstrates its potential with careful sample selection and nuanced interpretation, paving the way for further refinement and broader application.

Keywords. U–Pb dating, Dinosaur eggshell, Provence.

Funding. French Government, City of Aix-en-Provence (grant no. CIFRE 62/2008).

Note. Article submitted by invitation.

Manuscript received 21 November 2025, revised 12 March 2026, accepted 20 April 2026, online since 11 June 2026.

1. Introduction

Obtaining accurate chronostratigraphic constraints on continental deposits is challenging, necessitating innovative dating approaches. U–Pb dating applied to carbonate minerals has opened the possibility to date calcium carbonate $CaCO_3$ either in the form of calcite or aragonite (e.g. E. S. Smith and Farquhar, 1989; Rasbury and Cole, 2009). Dating based on isotopic dilution offers an accurate and precise analysis but is limited in application to relatively large samples (several mg) and requires a time consuming clean chemical preparation to avoid any Pb contamination (Woodhead and Petrus, 2019). Last decade

*Corresponding authors

#Contributed equally

developments in LA-ICP-MS allow sampling at high spatial resolution, down to ~0.1 mm, and fast data acquisition (Roberts et al., 2017). Several studies have attempted to date calcite fossils using LA-ICP-MS by focusing on early diagenesis mineral phases (e.g. Li et al., 2014; Rochín-Bañaga et al., 2024) showing the potential of U–Pb dating on such materials. This method has also proven to be reliable on less ideal fine grained carbonates (Montano et al., 2022) due to relatively high common Pb, and therefore relatively low $^{238}U/^{206}Pb$ which impacts age precision. This latter was recently applied in palustrine/lacustrine deposits in the Sainte-Victoire area allowing to refine the stratigraphy of those deposits (Roemers-Oliveira et al., 2024). Targeting biogenic carbonate minerals such as eggshells comes with issues associated with the effect of diagenesis on mobility of U and Pb. Ostrich eggshells U–Th dating carried out on modern and quaternary samples have shown that the eggshells behave as open systems for U and Th (Sharp et al., 2019; Loewy et al., 2020). However, recent studies by Chen et al. (2025) and Tucker et al. (2025) proposed the first dinosaurs eggshells U–Pb dating by LA-ICP-MS, suggesting that eggshells U and Pb systems could close in early diagenetic stages and thus approximate the hatching age. The present study is rooted in the same ongoing methodological exploration.

The Provence in southern France is famous for dinosaur eggs and nest outcrops. Philippe Matheron (1869) made the first record in the literature based on fragments collected in Rognac. The richness of Sainte-Victoire mountain foothills was really highlighted in the first half of the 20th century, with the first reports of de Lapparent (1947) from Roques-Hautes and Rousset (Bouches-du-Rhône), in addition of Fox-Amphoux (Var) areas. More recently, very important nesting sites were excavated in the city center of Aix-en-Provence (Garcia, Dutour, et al., 2003) and in the Réserve Naturelle de Sainte-Victoire, in the historic area of Roques-Hautes (Tortosa, 2014). In this later, the nests lagerstätte of Beaurecueil-Grands Creux 2, for example, has yielded more than 500 eggs, spatially organized in cluster of 2–7 eggs (study in progress). Those nests are observed in continental deposits, in reddish badlands formed by fine sandstones to claystones cut by sandstones channels rich in gravels corresponding to a fluvial plain environment. Those continental environments are often difficult to date due to the lack of biostratigraphical markers. Moreover, the sedimentation in these environments is spatially and stratigraphically discontinuous.

In the present study, we combine imaging techniques and LA-ICP-MS to identify zones with the best preservation in dinosaur eggshells collected in Campanian-Maastrichtian (83.6 ± 0.2 to 66.0 Ma) formations of Provence prior to U–Pb dating. This helps us to discuss the reliability of U–Pb dating by LA-ICP-MS application on dinosaur eggshells as well to better constrain continental deposit chronostratigraphy in the specific Provençal context.

2. Geological settings

2.1. *General context on Provence dinosaur eggs and nests*

As mentioned in Introduction, the Provence in southern France is famous for dinosaur eggs and nests with first record from Matheron (1869) and more extensive observations—notably in the Sainte-Victoire mountain surroundings—from de Lapparent (1947). Since then, many more nests have been discovered in the Réserve Naturelle de Sainte-Victoire (RNSV), most of those housed in the Museum of Natural History of Aix-en-Provence (MHNAix). Beyond these "nests", many more isolated eggshells were also collected making the Provence eggshell collection particularly rich. Most of those eggs—classified as Megaloolithidae in the literature (Vianey-Liaud, Mallan, et al., 1994)—were traditionally attributed to titanosaurian dinosaurs (Chiappe et al., 2003; Vila et al., 2010) but recent Romanian discoveries challenges this unique combination in associating it with basal hadrosaurids (Grigorescu et al., 2010). So, it is more parsimonious to envisage this oofamily associated with herbivorous dinosaurs, especially since *Rhabdodon* (Ornithopoda) was found as the most abundant dinosaur in local layers rich in megaloolithid eggs (despite the lack of non direct *in embryo* nor *in utero* discoveries).

In the Sainte-Victoire mountain foothills, the continental deposits were not directly dated but inferred from magnetostratigraphic studies combined with sedimentological analysis (Cojan and Moreau, 2006) and paleontological markers such as charophytes, ostracods, pollen, and gastropods surrounding the

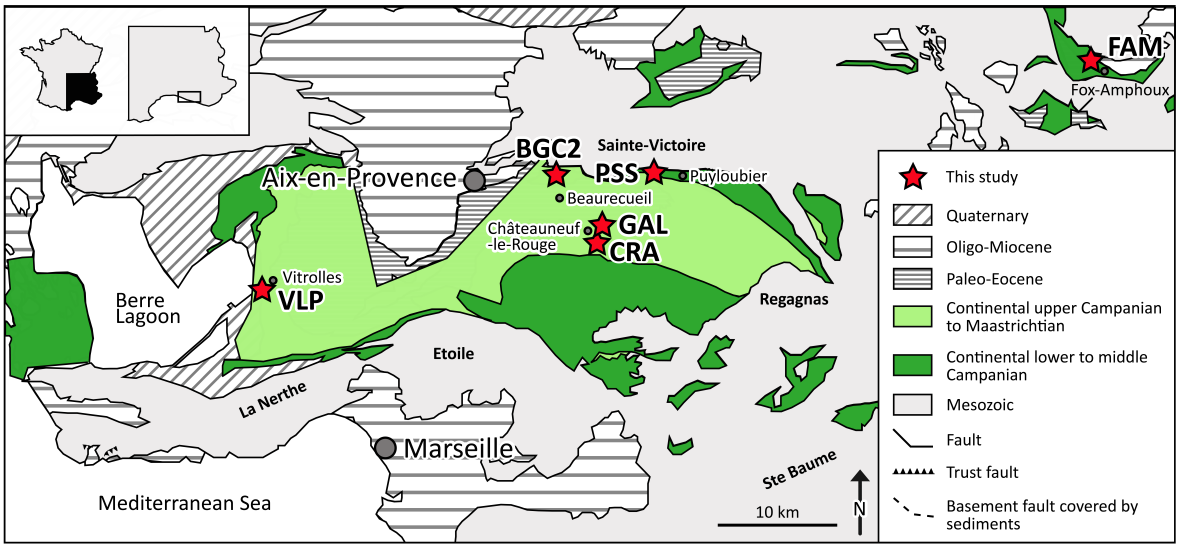

Figure 1. Geographical location of localities in this study in the continental Upper Cretaceous of Aix-en-Provence Basin with Beaurecueil—Grands Creux 2 (BGC2), Châteauneuf-le-Rouge—La Crau (CRA) and—La Galinière (GAL), Fox-Amphoux—Métisson (FAM), Puyloubier—Saint-Ser (PSS), Vitrolles—La Plaine (VLP).

interval rich in dinosaur eggshells (Babinot et al., 1983; Tortosa, 2014). However, thanks to the richness in eggshells, a local stratigraphy based on oospecies was proposed, increasing the precision of the scale but remaining still poorly anchored to the Geological Time Scale (Garcia and Vianey-Liaud, 2001) and highly dependent on the reliability and precision of determinations (Sellés, 2012; Dhiman et al., 2019; van der Linden et al., 2024).

2.2. *Sampling sites*

The dinosaur eggshells were collected in several places in Provence (Bouches-du-Rhône and Var departments), southern France (Figure 1).

2.2.1. *Beaurecueil—Grands Creux 2 (BGC2)*

Grands Creux 2 locality lies within the core restricted area of the Réserve Naturelle Sainte-Victoire (Beaurecueil, Bouches-du-Rhône department), at the foothill of the Montagne Sainte-Victoire, about 7 km east of Aix-en-Provence (Figure 1). This historical site, also known as Roques-Hautes, was discovered by de Lapparent (1947) and subsequently received considerable attention during the following decades for studies on dinosaur eggs (see Tortosa and Vianey-Liaud, 2021). It is located in the central part of the Aix-en-Provence Basin and belongs to the continental deposits historically referred to as the lower "*Argiles et Grès à Reptiles*" or lower "*Argiles Rutilantes*" Formation, dated to the upper Campanian (lower Rognacian local facies; Figure 2). In this area, the eggs—organized in nests—occur in floodplain fluvial deposits consisting of reddish siltstones to fine sandstones forming badland morphologies.

2.2.2. *Châteauneuf-le-Rouge—La Crau Autoroute (CRA)*

La Crau Autoroute locality (Châteauneuf-le-Rouge, Bouches-du-Rhône department) is located about 12 km southeast of Aix-en-Provence (Figure 1). This site was discovered in 2009 by the MHNAix during highway works for the widening of the A8 (Tabuce, Tortosa, et al., 2013; Tortosa, Buffetaut, et al., 2014; Tong et al., 2022). The site is located in the central part of the Aix-en-Provence Basin and belongs to the continental deposits historically referred to as the lower "*Argiles et Grès à Reptiles*" or lower "*Argiles Rutilantes*" Formation, dated to the upper Campanian (lower Rognacian local facies; Figure 2). The locality lies within floodplain deposits consisting of red clays interbedded with fluvial beds rich in bioclastic elements.

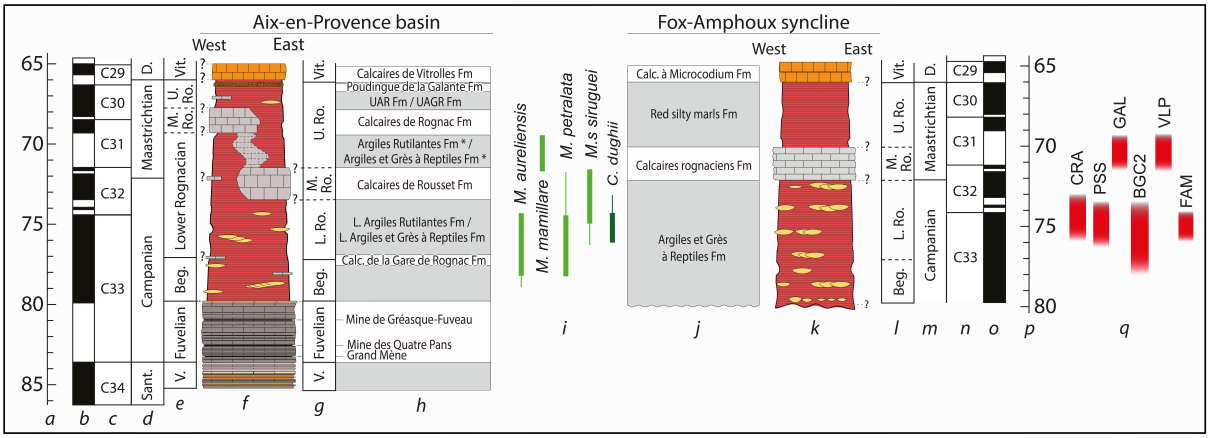

Figure 2. Chronostratigraphic position of the studied localities within a synthetic log of the continental Upper Cretaceous of Provence with time scale showing standard ages (*a*,*p*), geomagnetic polarity (*b*,*o*), polarity zones (*c*,*n*), stages (*d*,*m*), local continental facies (*e*,*g*,*l*), synthetic log of the Aix-en-Provence Basin and succession of formations (*f*,*h*), ootaxa stratigraphic distribution (*i*) and synthetic log of Fox-Amphoux syncline with succession of formations (*j*,*k*). Modified after Garcia and Vianey-Liaud (2001), Cojan and Moreau (2006), Tortosa (2014), Philip et al. (2017), Gradstein et al. (2020) and Tortosa and Leleu (2021). Abbreviations: Beg. = Begudian, D. = Danian, Sant. = Santonian, V. = Valdonnian, Vit. = Vitrollian.

2.2.3. *Châteauneuf-le-Rouge—La Galinière (GAL)*

La Galinière locality (Châteauneuf-le-Rouge, Bouches-du-Rhône department) is located about 13 km southeast of Aix-en-Provence (Figure 1). The presence of dinosaur eggs was officially recorded by a bailiff in 1977, which prevented the urbanization of the parcel. This locality was excavated in 2008 during a valorization campaign of paleontological localities carried out by the MHNAix within the Grand Site Sainte-Victoire labeled area. The outcrop is located in the central part of the Aix-en-Provence Basin and belongs to the continental deposits historically referred to as the upper "*Argiles et Grès à Reptiles*" or upper "*Argiles Rutilantes*" Formation, above the Calcaires de Rousset Formation and dated to the lower Maastrichtian (see middle part of Rognacian local facies; Figure 2). It consists of typical floodplain fluvial environments deposits, with reddish fine-grained sandstones, and contains several dinosaur egg clutches (interpreted here as nests).

2.2.4. *Fox-Amphoux—Métisson (FAM)*

Métisson locality (Fox-Amphoux, Var department) is located about 53 km east of Aix-en-Provence (Figure 1). It is a renowned locality for vertebrate discoveries (de Lapparent, 1947; Tortosa, 2014, for historical overview). The site is located within the Fox-Amphoux syncline and belongs to the continental deposits historically referred to as the "*Grès et Argiles à Reptiles*" Formation, dated to the upper Campanian (lower Rognacian local facies; Figure 2) (de Lapparent, 1947; Garcia and Vianey-Liaud, 2001; Cojan and Moreau, 2006; Tortosa, 2014). This formation is represented by approximately 300 m of alternating coarse sandstones, often conglomeratic, purple to pink marls, and marly limestones with pisoliths. The sandstones, with cross-bedding structures, are interpreted as fluvial channel fills, whereas the marls correspond to floodplain deposits.

2.2.5. *Puyloubier—Saint-Ser (PSS)*

Saint-Ser locality (Puyloubier, Bouches-du-Rhône department) is located at the foothill of the Sainte-Victoire mountain, about 16 km east of Aix-en-Provence (Figure 1). The outcrop was sampled in 2008 during a valorization campaign of paleontological localities carried out by the MHNAix within the Grand Site Sainte-Victoire labeled area, following initial reports from the 1980s. It is located in the eastern part of the Aix-en-Provence Basin and belongs to the continental deposits referred to as the lower "*Argiles et Grès à Reptiles*" or lower "*Argiles Rutilantes*" formations (Cojan and Moreau, 2006, Figure 2). The overlying limestone formation was recently distinguished from deposits observed

in the western part of the Aix-en-Provence Basin (Garcia and Vianey-Liaud, 2001; Tabuce, Tortosa, et al., 2013), and is here referred to the "*Calcaires de Rousset*" Formation, dated to the upper Campanian (Figure 2). The outcrop consists of a sandstone slab, lying a few meters below the limestone formation, on which several dinosaur egg sections are visible.

2.2.6. *Vitrolles—La Plaine (VLP)*

La Plaine locality (Vitrolles, Bouches-du-Rhône department) is located about 17 km southeast of Aix-en-Provence (Figure 1). The site is located in the western part of the Aix-en-Provence Basin and belongs to the continental deposits historically referred to as the lower "*Argiles et Grès à Reptiles*" or lower "*Argiles Rutilantes*" Formation (Tabuce, Vianey-Liaud, et al., 2004; Valentin et al., 2012). The outcrop consists of a succession of clays and mottled marls with interbedded sandstone lenses, overlain by the "*Calcaires de Rognac*" Formation.

Based on the stratigraphic distribution of ootaxa, Garcia and Vianey-Liaud (2001) demonstrated that this unit, also referred to as the "middle Rognacian" facies, is diachronous across the basin. In its western occurrences, the top of lower "*Argiles et Grès à Reptiles*" facies corresponds to the lower Maastrichtian whereas in its eastern counterparts, the base of the upper "*Argiles et Grès à Reptiles*" facies is of the same age (see the middle Rognacian local facies; Figure 2). The so-called "middle Rognacian" interval therefore represents a lacustrine carbonate facies developed between the base of the Calcaires de Rousset formation and the top of the "*Calcaires de Rognac*" formation (Tortosa, 2014; Turin, 2017).

3. Material and methods

3.1. *Sample collection*

A total of 10 eggshell samples were examined in this study. These specimens are curated in two public institutional collections: the Bouches-du-Rhône Departmental Collection (CD13) and the Muséum d'Histoire Naturelle d'Aix-en-Provence (MHNAix), France. Five eggshell samples originated from Beaurecueil—Grands Creux 2 (BGC2; Figure 1). Those eggshells were collected in 2017 during planned excavations conducted by the RNSV and MHNAix teams. The BGC2 series is housed in the CD13 collections, those also have a national collection number: BGC2.1A.2017.16 (collection number CD13-PV.2025.01.001), BGC2.1A.2017.32 (CD13-PV.2025.01.002), BGC2.1A.2017.49 (CD13-PV.2025.01.003), BGC2.1A.2017.51 (CD13-PV.2025.01.004) and BGC2.1A.2017.52 (CD13-PV.2025.01.005). The remaining specimens are curated in the MHNAix collections: one eggshell named hereafter CRA from Châteauneuf-le-Rouge—La Crau Autoroute (CRA in Figure 1) was collected from a complete egg (collection number MHNAIX.PV.2025.1.2). One eggshell named hereafter GAL is from Châteauneuf-le-Rouge—La Galinière (GAL in Figure 1), sampled from a complete egg (MHNAIX.PV.2025.10.1). One eggshell sample hereafter named FAM (collection number MHNA-PV.2005.24.18) is a subsample of eggs collected during excavation campaigns conducted by the MHNAix between 1997 and 2001 at Fox-Amphoux—Métisson (FAM; Figure 1). One eggshell named hereafter PSS (collection number MHNAIX.PV.2025.9.1) was collected from a sandstone slab from Puyloubier—Saint-Ser (PSS in Figure 1). Finally, the eggshell sample named hereafter VLP (collection number MHNA-PV.1999.13) is from Vitrolles—La Plaine (VLP in Figure 1) and was collected in 1999.

3.2. *Eggshells preparation*

To perform microscopic observations and geochemical analysis by LA-ICP-MS, the samples were mounted in radial section in a 1-inch resin epoxy plug—araldite 2020 produced by ESCIL. Once prepared, the radial section was polished in order to abrade any residual resin on the eggshell. The resin used is depleted in Pb and U, thus preventing any contamination of the sample.

3.3. *Eggshells optical microscopy, cathodoluminescence and numerical microscopy*

Eggshells were observed in optical microscopy with a binocular lens Leica M125 with a magnification from ×8 up to ×100 scale of observation commonly used for the parataxonomic assignment of dinosaur eggshells (Mikhailov, 1997). However, this scale and methodology was not adequate to fully explore the degree of preservation of the eggshell structures.

Table 1. Sample list classified based on U–Pb screening, analyses and ages calculation

Sample name	Localization	Oospecies	U–Pb screening ($^{238}U/^{206}Pb > 5$)	U–Pb analyses	U–Pb age
BGC.1A.2017.32 (CD13-PV.2025.01.002)	BGC2	*Megaloolithus* sp.	Not analyzed	-	-
BGC.1A.2017.49 (CD13-PV.2025.01.003)	BGC2	*M. petralta*	Not analyzed	-	-
BGC.1A.2017.51 (CD13-PV.2025.01.004)	BGC2	*M. petralta*	Not analyzed	-	-
BGC.1A.2017.16 (CD13-PV.2025.01.001)	BGC2	*M. petralta*	Not ok	-	-
BGC.1A.2017.52 (CD13-PV.2025.01.005)	BGC2	*M. petralta*	Not ok	-	-
GAL (MHN AIX.PV.2025.10.1)	GAL	*M. mamillare*	Not ok	-	-
FAM (MHNA-PV.2005.24.18)	FAM	*C. dughii*	Not ok	-	-
PSS (MHN AIX.PV.2025.9.1)	PSS	*M. siruguei*	Ok	$^{238}U/^{206}Pb < 10$	No
CRA (MHN AIX.PV.2025.1.2)	CRA	*C. dughii*	Ok	$^{238}U/^{206}Pb < 30$	Yes
VLP (MHNA-PV.1999.13)	VLP	*M. mamillare*	Ok	$^{238}U/^{206}Pb < 30$	Yes

All samples were studied with a cathodoluminescence installed on an optical microscope with ×4 and ×10 objectives and ×10 oculars. The microscope used was an Olympus BH-2, the cathodoluminescence a NewTec Scientific Cathodyne connected with an iDS camera. Depending on the luminescence of the eggshells, the electric potential was set between 12 kV and 18 kV, the intensity between 100 μA and 200 μA and 3 s photo acquisition time by default. Set of pictures after LA-ICP-MS analyses were performed using a Keyence VHX-7000 with magnification from ×30 up to ×300 under coaxial light.

3.4. *Eggshells SEM and EDS*

Before the preparation in plugs, BGC2.1A.2017.32, BGC2.1A.2017.51, CRA, GAL and FAM were observed with a SEM Hitachi S-3000N. Few uncalibrated EDS (Bruker Nano 129 eV XFlash Detector 5010) analyses were also performed on those samples with a range of spot analysis about few micrometers. These devices were used to identify minute structures and to observe possible chemical contamination or traces of diagenetic overprints. Sample VLP SEM images were taken after the U–Pb analyses.

3.5. *U–Pb analyses*

U–Pb analyses were carried out at CEREGE, Envitop Analytical facility, Aix-en-Provence, France, using an ESI 193 nm excimer laser ablation system coupled to an Element XR SF-ICP-MS (more detailed methodology and the U–Pb dataset are presented in supplementary material). At least 30 spots of 150 μm diameter were placed manually in zones showing the best preservation on cathodoluminescence images and having the highest U/Pb using quick laser ablation prescreening of Pb, U and Th signals. During prescreening, an empirical cut-off value for the $^{238}U/^{206}Pb$ of 5 is applied (Table 1). This value, although not very radiogenic for samples <100 Ma, allowed to quickly preselect zones with the best chance of providing spread in the $^{238}U/^{206}Pb$ ratios and hence U–Pb ages after data reduction.

After data acquisition, processing was done using Iolite (Paton et al., 2011) and an in-house excel spreadsheet to derive ages from Tera-Wasserburg diagrams using IsoplotR software (Vermeesch, 2018). WC1 was used as a primary standard to correct $^{238}U/^{206}Pb$ fractionation (Roberts et al., 2017) and AUG-B6 as a secondary standard to check for accuracy, yielding an age of 43 ± 2 Ma in agreement with Pagel et al. (2018). Ages are quoted at a 2s, including the propagation of systematic uncertainty of the standards following (Horstwood et al., 2016).

For LA-ICP-MS elemental mapping, a square spot size of 100 μm, raster speed, and MS cycling time were synchronized to provide low-resolution images with 100 μm^2 pixels, sufficient to correlate these

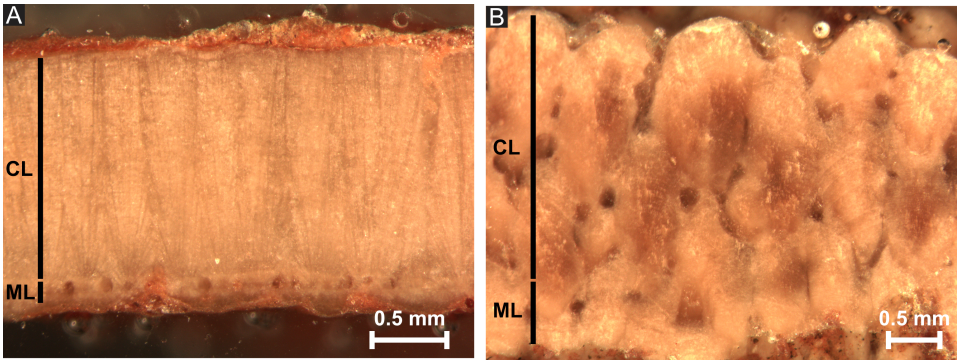

Figure 3. Radial section observation of calcite structure of (A) sample BGC2.1A.2017.51 *M. petralta* and (B) sample PSS *M. siruguei*. CL—continuous layer and ML—mammillary layer.

mappings to other imagery techniques used in this study. A JCp*-1-NP pellet from myStandards GmbH was used as a reference.

4. Results

4.1. *Egg shells oospecies identification, microstructure, preservation and contamination*

Typical structures of eggshells were observed in optical microscopy based on radial sections and complementary information were made based on the sculpture of the outer surface. Shell units were discretispherulitic (or tubospherulitic) with ovoid mammilla and radial-tabular columns (Mikhailov, 1997, Figure 3A). The spaces between the mammila were filled with sediments with a different color and texture than the shell itself. The discretispherulitic structure confirmed the attribution to Megaloolithidae oofamily. Pore canals were not easily observed in most samples, with the exception of FAM and PSS which had tubocanaliculate pore canals (Figure 3B). In many samples—when visible—the outer face of the egg was covered by nodes. The proximal face was smooth—when not encrusted. More precisely, BGC2.1A.2017.16 (Supplementary Figure 1), BGC2.1A.2017.49, BGC2.1A.2017.51 (Figure 3A) and BGC2.1A.2017.52 (Supplementary Figure 2) were attributed to the oospecies *Megaloolithus petralta* (Vianey-Liaud, Mallan, et al., 1994) based on the node diameter (0.4–0.6 mm), its slightly arched growth lines, and partially fused, narrow fan-shaped shell units. The sample BGC2.1A.2017.32 was tentatively attributed to *Megaloolithus* sp. Although historically attributed to *Megaloolithus aureliensis* (ibid.) and later to *Megaloolithus* cf. *aureliensis* (Vianey-Liaud and Garcia, 1999), it is now regarded as a distinct oospecies with a smaller general size, thinner shell thickness, arched growth lines, and partially fused fan-shaped shell units. So far, *Megaloolithus* sp. was exclusively reported from BGC2 locality. The sample GAL (Supplementary Figure 3) from Châteauneuf-le-Rouge—La Galinière and the sample VLP from Vitrolles—La Plaine were attributed to the oospecies *Megaloolithus mamillare* (Vianey-Liaud, Mallan, et al., 1994) based on arched growth lines following the surface and unfused short and broadly fan-shaped shell units. The sample PSS (Supplementary Figure 4) from Puyloubier—Saint-Ser was attributed to the oospecies *Megaloolithus siruguei* (ibid., Figure 3B), with strongly arched growth lines, unfused fan-shaped shell units, and a reticulate canal pore system. Finally, the samples CRA (Châteauneuf-le-Rouge—La Crau Autoroute) and FAM (from Fox-Amphoux—Métisson; Supplementary Figure 5) were attributed to the oospecies *Cairanoolithus dughii* (ibid.) based on horizontal growth lines in the interlocking shell units and more arched single units as well as the presence of very smooth nodes on the external surface. The Supplementary Figure 6 summarizes the oospecies identifications.

SEM pictures of sample CRA *C. dughii*, sample GAL *M. mamillare*, sample FAM *C. dughii*, sample BGC2.1A.2017.32 *Megaloolithus* sp. and sample BGC2.1A.2017.51 *M. petralta* showed that the

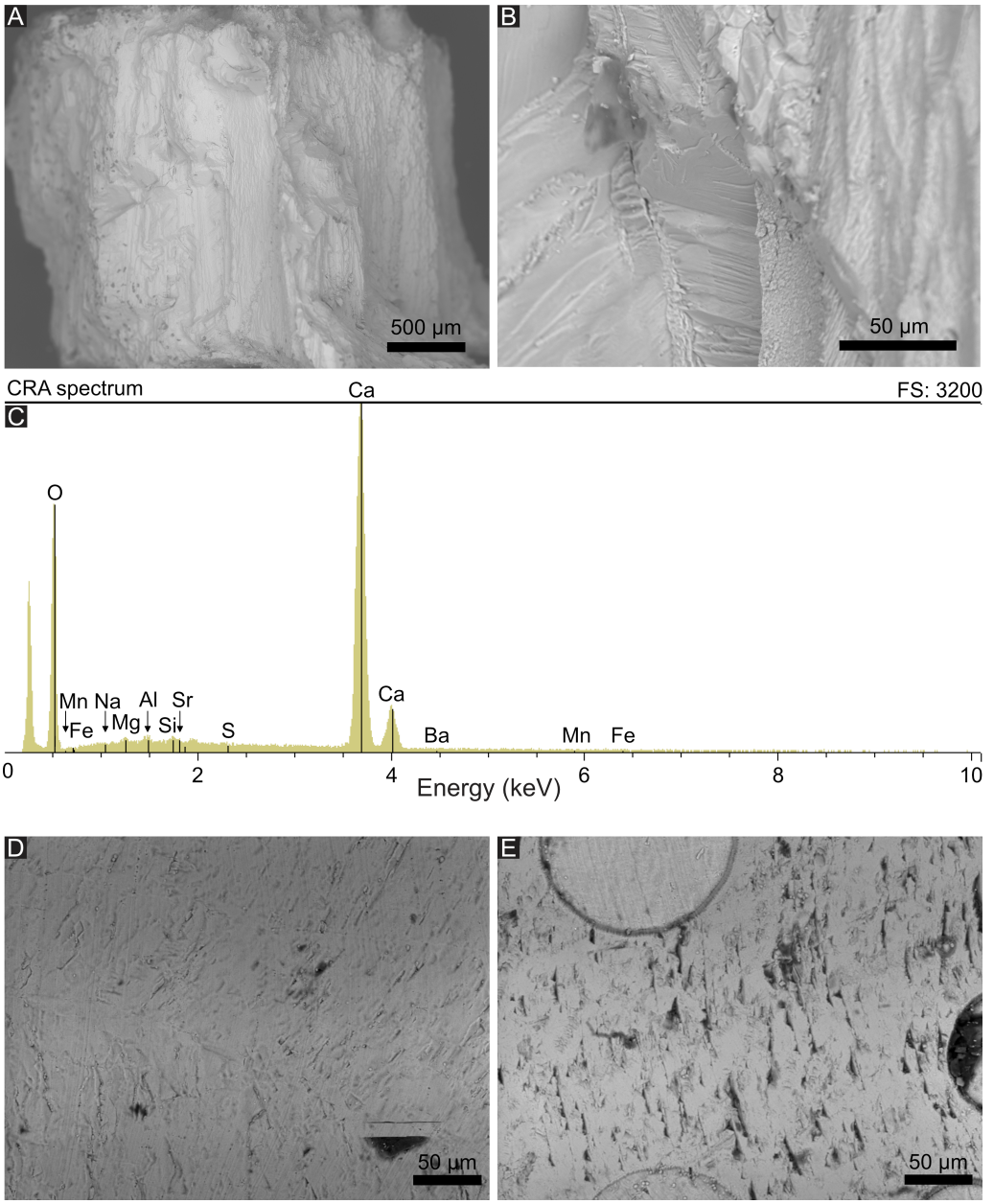

Figure 4. (A,B) SEM picture of sample CRA *C. dughii* (CRA). (C) EDS spectrum of sample CRA *C. dughii* calcite. (D,E) SEM pictures of sample VLP *M. mamillare.*

prismatic structure of the thick $CaCO_3$ layer was preserved (Figure 4 and Supplementary Figures 7–10). The cathodoluminescence showed that recrystallisation and secondary crust were luminating (Figures 5, 6 and Supplementary Figures 7–10). Those were concentrated in the inner and outer faces of eggshells, probably due to the contribution of clays. In most case, luminescence was observed between two shell units, within radial thin structures. If some of those structures may correspond to pore canals (Supplementary Figure 4), in most case those seemed too narrow to correspond to tubocanals and thus may

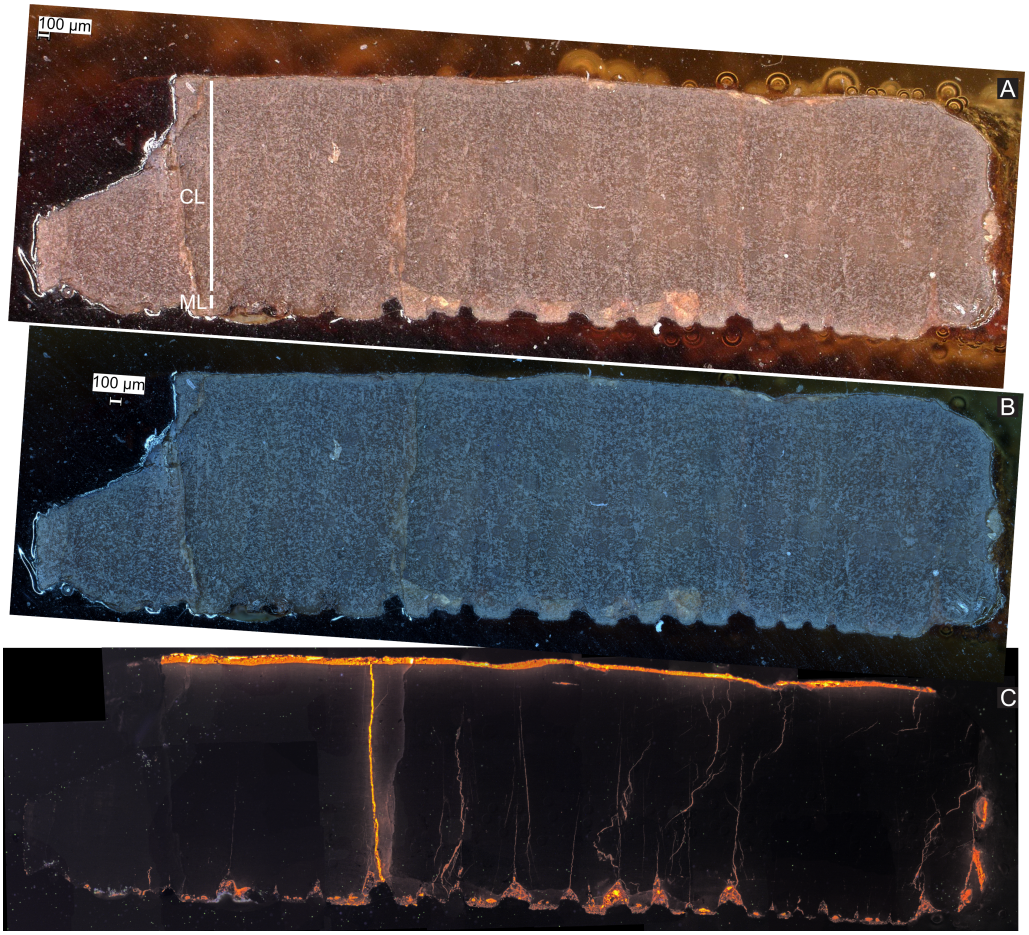

Figure 5. Sample CRA *C. dughii* pictures (A) in natural light (×30 magnification); (B) natural light high magnification panorama (×150 magnification); (C) cathodoluminescence. CL—continuous layer and ML—mammillary layer.

correspond to fractures and/or interface between two shell units (Figure 5 and Supplementary Figure 1). In PSS (Supplementary Figure 4), the pore canals displayed circularly banded luminescence interpreted as recrystallisation within the pores.

Most of the prismatic calcite forming the majority of the eggshell was depleted in transition metals (Figure 4 and Supplementary Figures 7–10) and did not present any luminescence (Figures 5, 6 and Supplementary Figures 1, 2, 5). To conclude, the faces, thin fractures, transversal canal pores, and longitudinal pores were encrusted with clays and/or $CaCO_3$ enriched in transition metals testifying secondary crystallization. The rest of the prismatic layer showed comparatively a better preservation and was targeted for laser ablation analyses.

4.2. *U–Pb–Th concentrations*

Elemental mapping (LA-ICP-MS) of sample VLP showed distinct spatial distributions of Mn (not shown), Pb, Th, U. Concentrations ranged from 0 to 150 ppm, 50 ppm, 1.5 ppm, 10 ppm respectively (Figure 7). The highest values for all elements occurred near sutures and in the inner and outer layers, which were interpreted as zones enriched in clays and/or affected by diagenetic processes. In contrast, the prismatic calcite outside these areas exhibited significantly lower concentrations (Th $\ll$ 0.5 ppm, Pb $\ll$ 1 ppm, U $\ll$ 1 ppm), suggesting minimal contamination and secondary alteration—consistent with observations from cathodoluminescence imaging. $^{238}U/^{206}Pb$ varied from 0 to ~25 with the most

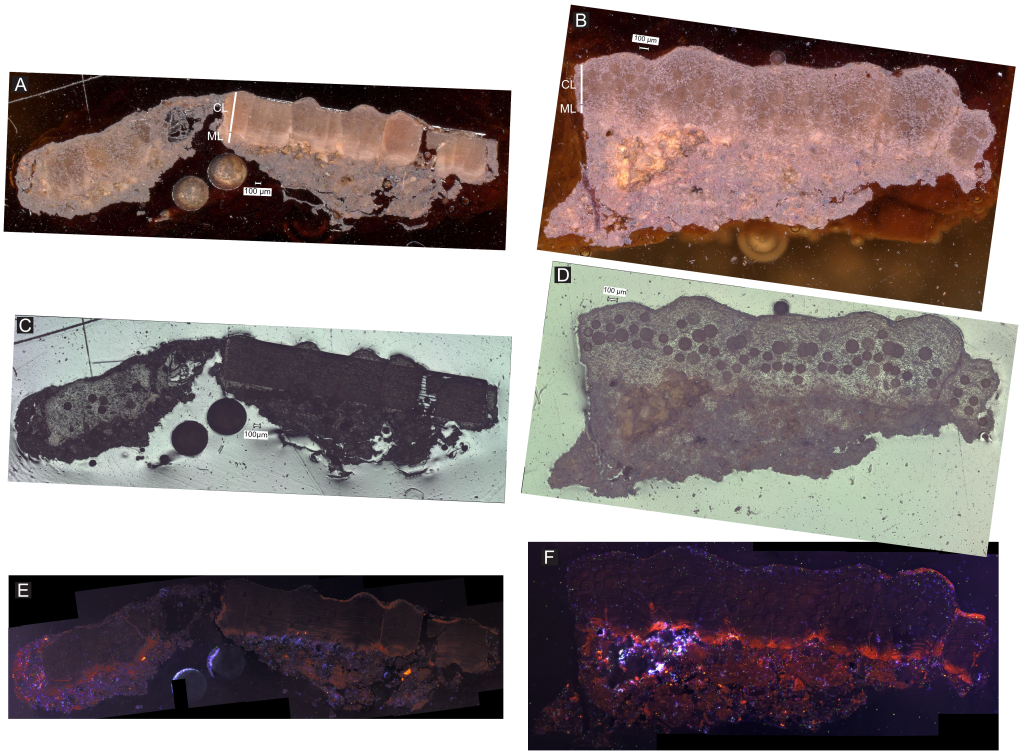

Figure 6. Sample VLP *M. mamillare* pictures (A,B) in coaxial light high magnification panorama (×150 magnification); (C,D) in natural light (×30 magnification); (E,F) cathodoluminescence. Circles on the sample are the trace of the laser ablation. CL—continuous layer and ML—mammillary layer.

radiogenic values (highest ratios) found in areas with the lowest Pb and U concentrations. Age calculation from the elemental mapping could not be applied due the overall low Pb content in the best-preserved zones that prevented the use of ^{207}Pb measurements, as the signal on the 207 mass was too low to be reliable.

4.3. *U–Pb ages*

Only two samples, CRA and VLP, yielded reliable U–Pb isochrons (Figure 8). Some other samples were tested (see Table 1), but did not yield reliable isochrons mainly due to unfavorable ^{238}U/^{206}Pb ratios—below the cut-off value of 5—and excluded to the exception of sample PSS presented in Supplementary Figure 11. The age of sample VLP attributed to *Megaloolithus mamillare* was calculated to 67.4 ± 4.4 Ma (2s, n = 60) (Figure 8A). The age of sample CRA attributed to *Cairanoolithus dughii* was calculated to 69.5 ± 9.9 (2s, n = 50) (Figure 8B). Considering the uncertainties, sample VLP was dated within the Maastrichtian-Danian (Paleocene) time interval and sample CRA within the Campanian-Selandian (Paleocene) time interval. Since these eggshells coming from dinosaur species cannot be younger than the Cretaceous–Paleogene (K–Pg) boundary, VLP age's was considered Maastrichtian and CRA Campanian to Maastrichtian. For both samples, the ^{238}U/^{206}Pb were relatively low (<35) compared to the ^{238}U/^{206}Pb radiogenic concordia intercept of ~100 for ages ~68 Ma, leading to moderate uncertainties (6.5% and 15%, respectively). Based on LA-ICP-MS, CRA had lower Pb concentrations and lower U concentrations (<100 ppb in average for both Pb and U) compared to VLP (~500 ppb in average for both Pb and U) which explain its greater uncertainty despite showing a similar ^{238}U/^{206}Pb range. For each sample, the initial ^{207}Pb/^{206}Pb ~0.84 was consistent with the expected value of less than 100 Ma formations (Stacey and Kramers, 1975). The ^{232}Th concentrations were well below 0.5 ppm (Figure 7) limiting the possible contamination from secondary phases (see previous section).

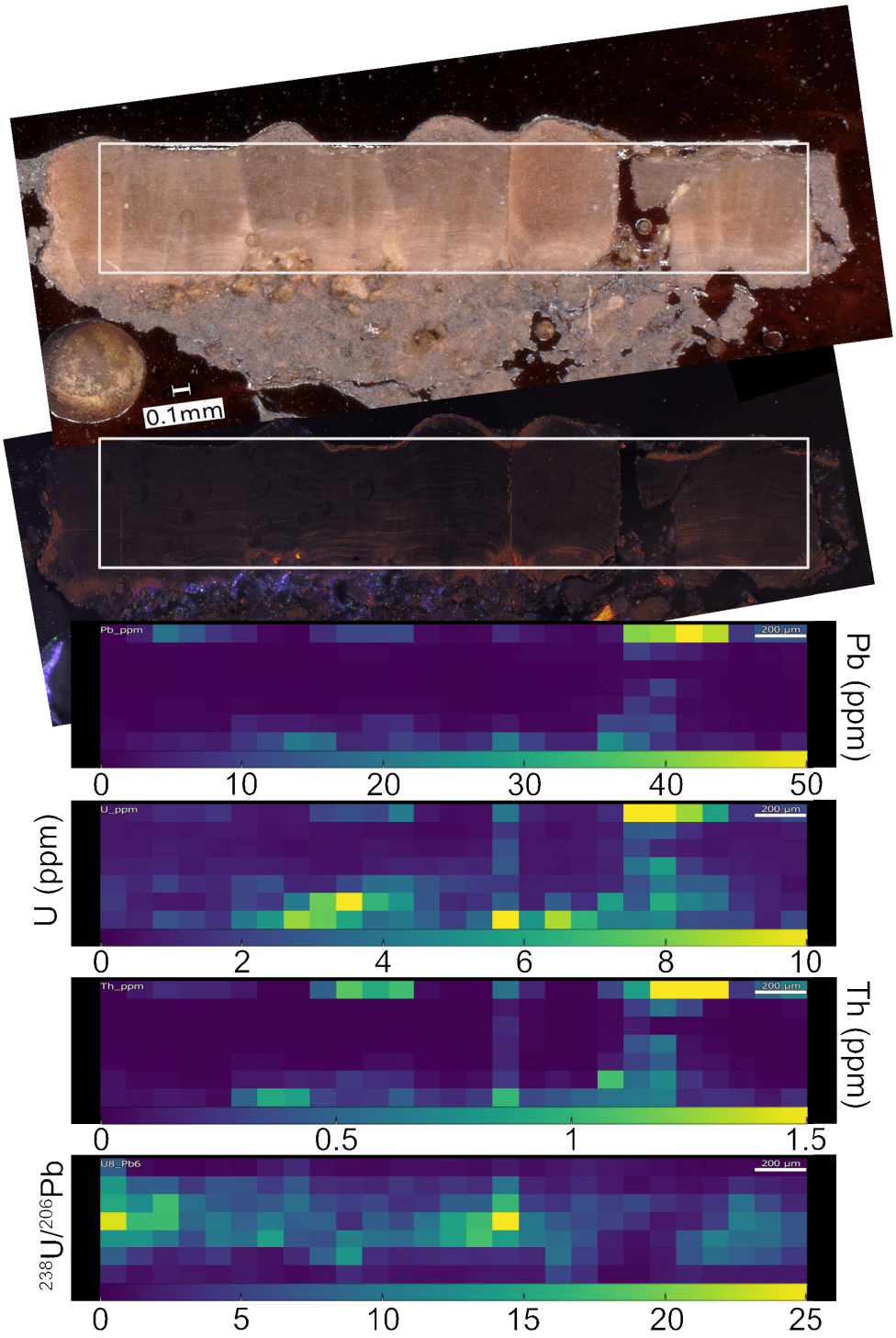

Figure 7. Low resolution (1 pixel = 100 µm^2) elemental and $^{238}U/^{206}Pb$ mapping of sample VLP *M. mamillare* showing low concentration of detrital elements such as ^{232}Th in the prismatic calcite zones. Circles on the sample are the trace of the laser ablation.

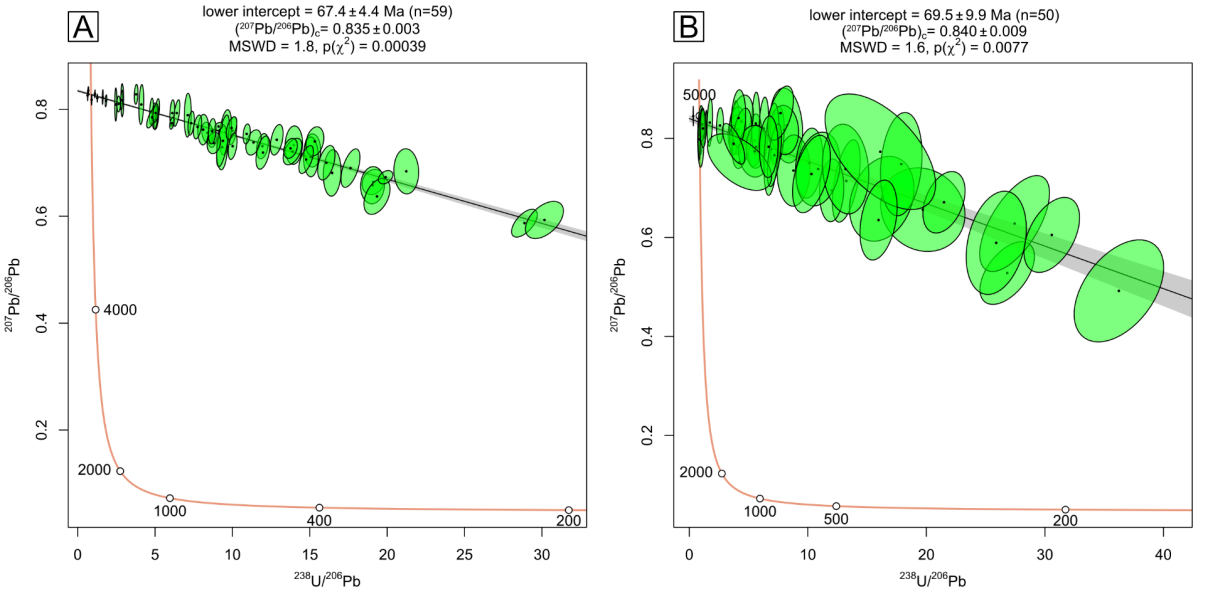

Figure 8. Tera-Wasserburg diagram of the U–Pb data of sample VLP (A) and CRA (B). The uncertainty on the age includes the propagation of systematic uncertainties of the standards as specified in the supplementary material.

5. Discussion

5.1. *U–Pb system in eggshells and diagenesis*

Previous U–Th analyses of Quaternary ostrich eggs showed that the prismatic calcite forming the shell behaved as an open U-series system, requiring advection–diffusion models to account for U mobility during diagenesis and to derive ^{230}Th–U ages estimates (Sharp et al., 2019). On U–Pb timescales, it can be expected that the U-series system was subject to several post-depositional processes, including contamination from soil-derived detrital particles filling in the intercrystalline microporosity of the eggshell (Loewy et al., 2020) and/or mobility of U and Pb, potentially driven by meteoric or sediment derived fluids circulation along pores or microfractures of the shells (Tucker et al., 2025). The time scale for which the U-series system in prismatic calcite remains open is still an open question and hence U–Pb ages must be considered as minimum ages. Tucker et al. (ibid.) demonstrated that U–Pb ages obtained from dinosaur eggshells in the Western Interior Basin of the USA—where preservation was rigorously controlled through both optical and geochemical analyses—agree within a 5% margin with Maximum Deposition Ages derived from detrital zircons. In the samples studied here, elemental mapping (Figure 7) defined two zones with distinct spatial distribution of U and ^{238}U/^{206}Pb. The first one, corresponding to the inner and outer layers as well as the fractures and pores, was characterized by variable and high U and Th contents, along with high Mn and Pb and low ^{238}U/^{206}Pb. This zone showed evidence of contamination with detrital material in both optical and cathodoluminescence images. The second zone, located in the core of the prismatic calcite, exhibited lower U (<1 ppm), Th, Mn and Pb and relatively high and variable ^{238}U/^{206}Pb ratios. Optical and cathodoluminescence imaging indicated that this zone was well preserved.

U–Pb spot analyses in the well-preserved prismatic calcite of samples VLP and CRA define Tera-Wasserburg diagrams with robust linear alignment and consistent intercept ages (Figure 8). These results demonstrate that the U–Pb system remained closed for approximately 68 Ma in both samples. Notably, both samples exhibit limited radiogenic ingrowth, as evidenced by ^{238}U/^{206}Pb below 30—significantly lower than the expected radiogenic intercept of around 100 for 68 Ma Tera-Wasserburg isochron (Supplementary Figure 12). Similar ^{238}U/^{206}Pb ranges were reported by Chen et al. (2025) and Tucker et al. (2025) for samples

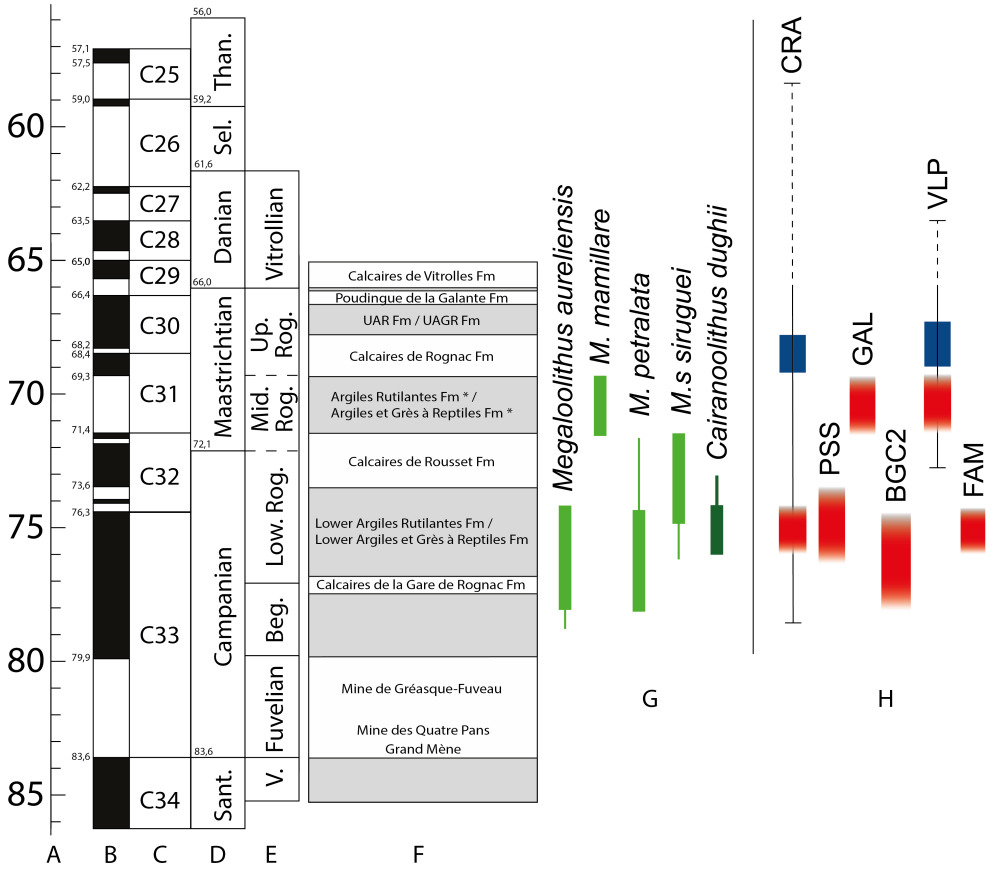

Figure 9. Stratigraphic position of the studied localities (H) in time scale showing standard ages (A), geomagnetic polarity (B), polarity zones (C), stages (D), local continental facies (E), succession of continental formations withing Aix-en-Provence Basin (F) and ootaxa stratigraphic distribution (G), modified after Garcia and Vianey-Liaud (2001), Cojan and Moreau (2006), Tortosa (2014), Philip et al. (2017), Gradstein et al. (2020) and Tortosa and Leleu (2021). Radiometric U–Pb ages (blue boxes) and the repositioning of localities based on the biostratigraphic synthesis (red boxes). Abbreviations: Beg. = Begudian, D. = Danian, Sant. = Santonian, Sel. = Selandian, Than. = Thanetian, V. = Valdonnian, Vit. = Vitrollian.

aged between 95 and 66 Ma from diverse continental settings. These consistencies in $^{238}U/^{206}Pb$ are interpreted as indicative of a shared mechanism of U incorporation during early diagenesis in the prismatic calcite of dinosaur eggshells.

U sensitivity to redox conditions influences its geochemical behavior and mobility during diagenesis (Langmuir, 1978), in contrast to Pb. Modern avian eggs incorporate negligible U during calcification (U <1 ppt) (Loewy et al., 2020), and arguably this can be speculated to apply to non-avian dinosaur eggs. Post-depositional incorporation of U in $CaCO_3$ (as UO_2^{2+}) would require calcite dissolution-precipitation (Reeder et al., 2001), which is inconsistent with the pristine mineralogical preservation observed in optical, SEM, and cathodoluminescence images of the well-preserved zones. Avian eggshells also contain significant amounts of organic matter, such as proteins, that impregnate the calcite matrix (D. L. Smith and Hayward, 2010). Given that tetravalent U(IV) has a known affinity for organic matter (Bone et al., 2017), the presence and spatial distribution of the organic phase—though not analyzed during this study—could explain both the observed heterogeneity in U distribution and the long-term stability of the U–Pb system. If U uptake within the eggshell is controlled by the early diagenesis of organic matter intertwined with calcite, U uptake would be inherently linked to the bio-mineralogical composition of the shell and its

interaction with external factors such as meteoritic or sediment-driven fluid circulation. U uptake would not need dissolution–reprecipitation to take place. This mechanism could greatly expand the applicability of U–Pb dating of dinosaur eggshells in other continental deposits, as also demonstrated by the successful results published by Chen et al. (2025) and Tucker et al. (2025).

5.2. *Consistency of the U–Pb ages with stratigraphy of the sampling sites*

The two U–Pb ages are consistent with each other, with a combined age of 67.7 ± 4.2 Ma (2s, n = 110) (see also Supplementary Figure 13), and both align with the stratigraphic age derived from independent markers (Figure 9). However, while these U–Pb ages are broadly consistent with the expected ca. 70 Ma range, their uncertainties, reaching up to 15% due to relatively low $^{238}U/^{206}Pb$ and low U and Pb contents, remain too large to resolve detailed stratigraphic relationships. The U–Pb ages obtained are less precise than the local stratigraphy. Although stratigraphy in continental deposits are often less precise than in marine deposits, the Provence region gathered almost 80 years of litho-, bio- and magnetostratigraphy literature limiting the input of calcite U–Pb ages. Together with the limited range in $^{238}U/^{206}Pb$ and the low success rate discussed in the previous section, these results highlight both the promise and current limitations of the method. In cases where dinosaur eggshells are the only available biostratigraphic markers, U–Pb analyses could provide a valuable complementary approach to microstructural studies and possible age anchors in the regional stratigraphy. Nevertheless, such analyses require thorough assessment of sample preservation before conducting in situ U–Pb measurements, similarly to results of Tucker et al. (ibid.).

6. Conclusion

U–Pb dating by LA-ICP-MS was tested on Provence dinosaur eggshells. Prior to chemical analyses, a combination of optical, SEM and cathodoluminescence observations allowed to identify potential contamination from detrital and secondary mineralogical phases in borders, fractures, pores, and even within the calcite for some samples. Over the whole set tested (seven samples), only two yielded statically robust ages, although with elevated uncertainty (up to 16%). These ages, nevertheless, are broadly consistent with the independent stratigraphic framework for the study sites. The results produced in this study showed that U–Pb dating can be applied to non-avian dinosaur eggshells—similarly to very recent publications. It also highlights that it is critical to conduct a thorough determination of preservation of the eggshells with optical, SEM and cathodoluminescence microscopy prior to conducting U–Pb analyses.

Altogether, this study shows that, despite a low success rate, U–Pb dating of dinosaur eggshells holds significant potential. When combined with microstructural, paleontological, and stratigraphic markers, it provides a complementary approach for constraining the temporal framework of continental successions that otherwise remain poorly anchored to the global time scale. Without any other stratigraphic markers, the application of this method is even more attractive to estimate the age of the eggshells and the surrounding sediment. These results pave the way for further applications on other Upper Cretaceous localities in Europe and beyond.

CRediT authorship contribution statement

Abel Guihou: Conceptualization, Formal analysis, Investigation, Methodology, Resources, Validation, Visualization, Writing—original draft, Writing—review & editing.
Baptiste Suchéras-Marx: Conceptualization, Investigation, Project administration, Validation, Visualization, Writing—original draft, Writing—review & editing.
Thierry Tortosa: Investigation, Resources, Visualization, Writing—original draft, Writing–review & editing.
Pierre Deschamps: Resources.
Yves Dutour: Resources.

Acknowledgments

We warmly thanks Julien Longerey for the preparation of the plugs and help with the SEM. U–Pb analyses were performed at CEREGE by equipment acquired in the frame of the Initiative d'Excellence of

Aix-Marseille University—A*Midex, DatCarb project. We gratefully acknowledge the Département des Bouches-du-Rhône and J.-M. Perrin, its elected representative for the promotion of Provence's paleontological and archaeological heritage, for their continuous support, excavation authorization, and administrative assistance. We are also indebted to the Direction de l'Environnement, des Grands Projets et de la Recherche (E. Mangion, H. Souan, M. Bourrelly) and and numerous volunteers during the field campaigns on the Réserve Naturelle de Sainte-Victoire for their help in the field and logistical coordination since 2015. We further thank the staff of the Muséum d'Histoire Naturelle d'Aix-en-Provence (S. Berton, M. Desparoir, Nicolas Vialle, Eric Turini). Part of TT's work was supported by a PhD CIFRE 62/2008 grant from the French government and the city of Aix-en-Provence. Finally, we thanks the two anonymous reviewers and the editorial team for their comments that greatly improved the manuscript.

Declaration of interests

The authors do not work for, advise, own shares in, or receive funds from any organization that could benefit from this article, and have declared no affiliations other than their research organizations.

Supplementary materials

Supporting information for this article is available on the journal's website under https://doi.org/10.5802/crgeos.338 or from the author.

References

Babinot, J.-F., J. P. Bellier, M. Bilotte, et al., "Conclusions au colloque sur les étages Coniacien à Maastrichtien : échelles biostratigraphiques", *Géol. Méditerranéenne* **10** (1983), pp. 413–434.

Bone, S. E., J. J. Dynes, J. Cliff and J. R. Bargar, "Uranium(IV) adsorption by natural organic matter in anoxic sediments", *Proc. Natl. Acad. Sci. USA* **114** (2017), pp. 711–716.

Chen, Q., X. Cheng, J. Wang, et al., "Geological age of the Yunyang dinosaur eggs revealed by in-situ carbonate U–Pb dating and its scientific implications", *Front. Earth Sci.* **13** (2025), article no. 1638838.

Chiappe, L. M., R. A. Coria, F. Jackson and L. Dingus, "The Late Cretaceous nesting site of Auca Mahuevo (Patagonia, Argentina): eggs, nests, and embryos of titanosaurian sauropods", *Palaeovertebrata* **32** (2003), pp. 97–108.

Cojan, I. and M.-G. Moreau, "Correlation of terrestrial climatic fluctuations with global signals during the upper Cretaceous–Danian in a compressive setting (Provence, France)", *J. Sedim. Res.* **76** (2006), pp. 589–604.

Dhiman, H., G. V. R. Prasad and A. Goswami, "Parataxonomy and palaeobiogeographic significance of dinosaur eggshell fragments from the Upper Cretaceous strata of the Cauvery Basin, South India", *Hist. Biol.* **31** (2019), pp. 1310–1322.

Garcia, G., Y. Dutour, I. Cojan, I. Cojan, X. Valentin and G. Cheylan, "Long-term fidelity of megaloolithd egg-layers to a large breeding-ground in the Upper Cretaceous of Aix-en-Provence (Southern France)", *Palaeovertebrata* **32** (2003), pp. 109–120.

Garcia, G. and M. Vianey-Liaud, "Dinosaur eggshells as biochronological markers in Upper Cretaceous continental deposits", *Palaeogeogr. Palaeoclimatol. Palaeoecol.* **169** (2001), pp. 153–164.

Gradstein, F. M., J. G. Ogg, M. B. Schmitz and G. M. Ogg, *The Geologic Time Scale 2020*, Elsevier: Amsterdam, 2020, p. 1357.

Grigorescu, D., G. Garcia, Z. Csiki, V. Codrea and A.-V. Bojar, "Uppermost Cretaceous megaloolithid eggs from the Haţeg Basin, Romania, associated with hadrosaur hatchlings: search for explanation", *Palaeogeogr. Palaeoclimatol. Palaeoecol.* **293** (2010), pp. 360–374.

Horstwood, M. S. A., J. Košler, G. Gehrels, et al., "Community-derived standards for LA-ICP-MS U-(Th-)Pb geochronology — uncertainty propagation, age interpretation and data deporting", *Geostand. Geoanal. Res.* **40** (2016), pp. 311–332.

Langmuir, D., "Uranium solution-mineral equilibria at low temperatures with applications to sedimentary ore deposits", *Geochim. Cosmochim. Acta* **42** (1978), pp. 547–569.

de Lapparent, A. F., "Les dinosauriens du Crétacé supérieur du Midi de la France", *Mém. Soc. Géol. Fr.* **56** (1947), pp. 1–67.

Li, Q., R. R. Parrish, M. S. A. Horstwood and J. M. McArthur, "U–Pb dating of cements in Mesozoic ammonites", *Chem. Geol.* **37** (2014), pp. 76–83.

van der Linden, T. T. P., D. K. Zelenitsky, R. H. B. Fraaije, G. Garcia, X. Valentin, F. M. Holwerda and A. S. Schulp, "The first hadrosauroid eggshell from the Aix-en-Provence Basin (late Maastrichtian) of France", *Hist. Biol.* **37** (2024), pp. 1435–1442.

Loewy, S. L., J. Valdes, H. Wang, et al., "Improved accuracy of U-series and radiocarbon dating of ostrich eggshell using a sample preparation method based on microstructure and geochemistry: a study from the Middle Stone Age of Northwestern Ethiopia", *Quat. Sci. Rev.* **247** (2020), article no. 106525.

Matheron, P., "Note sur les reptiles fossiles des dépôts fluvio-lacustres crétaces du bassin à lignite de Fuveau", *Bull. Soc. Geol. Fr.* **2** (1869), no. 26, pp. 781–795.

Mikhailov, K. E., "Fossil and recent eggshell in amniotic vertebrates: fine structure, comparative morphology and classification", *Spc. Pap. Palaeontol.* **56** (1997), pp. 1–80.

Montano, D., M. Gasparrini, S. Rohais, R. Albert and A. Gerdes, "Depositional age models in lacustrine systems from zircon and carbonate U–Pb geochronology", *Sedimentology* **69** (2022), pp. 2507–2534.

Pagel, M., M. Bonifacie, D. A. Schneider, et al., "Improving paleohydrological and diagenetic reconstructions in calcite veins and breccia of a sedimentary basin by combining Δ_{47} temperature, $\delta_{18}O_{water}$ and U–Pb age", *Chem. Geol.* **481** (2018), pp. 1–17.

Paton, C., J. Hellstrom, B. Paul, J. Woodhead and J. Hergt, "Iolite: freeware for the visualisation and processing of mass spectrometric data", *J. Anal. At. Spectrom.* **26** (2011), pp. 2508–2518.

Philip, J., M. Vianet-Liaud, C. Martin-Closas, R. Tabuce, P. Léonide, J.-P. Margerel and J. Noël, "Stratigraphy of the Haut Var Paleogene continental series (Northeastern Provence, France): new insight on the age of the 'Sables bleutés du Haut Var' Formation", *Geobios* **50** (2017), pp. 319–339.

Rasbury, E. T. and J. M. Cole, "Directly dating geologic events: U–Pb dating of carbonate", *Rev. Geophys.* **47** (2009), article no. RG3001.

Reeder, R. J., M. Nugent, C. D. Tait, D. E. Morris, S. M. Heald, K. M. Beck, W. P. Hess and A. Lanzirotti, "Coprecipitation of uranium(VI) with calcite: XAFS, micro-XAS, and luminescence characterization", *Geochim. Cosmochim. Acta* **65** (2001), pp. 3491–3503.

Roberts, N. M. W., E. T. Rasbury, R. R. Parrish, C. J. Smith, M. S. A. Horstwood and D. J. Condon, "A calcite reference material for LA-ICP-MS U–Pb geochronology", *Geochem. Geophys. Geosyst.* **18** (2017), pp. 2807–2814.

Rochín-Bañaga, H., D. W. Davis and J. Moysiuk, "U–Pb dating of belemnites and rugose corals: the potential for absolute dating of calcitic invertebrate fossils", *Chem. Geol.* **644** (2024), article no. 121862.

Roemers-Oliveira, E., F. Fournier, S. Viseur, et al., "The anatomy and stacking pattern of palustrine-dominated carbonate sequences from the Cengle Plateau, Paleocene, SE France: a multi-scalar approach", *Sediment. Geol.* **470** (2024), article no. 106690.

Sellés, A. G., *Oological record of dinosaurs in South-Central Pyrenees (SW Europe): parataxonomy, diversity and biostratigraphical implications*, PhD thesis, Universität de Barcelona: Barcelona (Spain), 2012. p. 237.

Sharp, W. D., C. A. Tryon, E. M. Niespolo, N. D. Fylstra, A. Tripathy-Lang and J. T. Faith, "^{230}Th/U burial dating of ostrich eggshell", *Quat. Sci. Rev.* **219** (2019), pp. 263–276.

Smith, D. L. and J. L. Hayward, "Bacterial decomposition of avian eggshell: a taphonomic experiment", *Palaios* **25** (2010), pp. 318–326.

Smith, E. S. and R. M. Farquhar, "Direct dating of Phanerozoic sediments by the ^{238}U–^{206}Pb method", *Nature* **341** (1989), pp. 518–521.

Stacey, J. S. and J. D. Kramers, "Approximation of terrestrial lead isotope evolution by a two-stage model", *Earth Planet. Sci. Lett.* **26** (1975), pp. 207–221.

Tabuce, R., T. Tortosa, M. Vianey-Liaud, et al., "New eutherian mammals from the Late Cretaceous of Aix-en-Provence Basin, south-eastern France", *Zool. J. Linn. Soc.* **169** (2013), pp. 653–672.

Tabuce, R., M. Vianey-Liaud and G. Garcia, "A eutherian mammal in the latest Cretaceous of Vitrolles, southern France", *Acta Palaeontol. Pol.* **49** (2004), pp. 347–356.

Tong, H., T. Tortosa, E. Buffetaut, Y. Dutour, E. Turini and J. Claude, "A compsemydid turtle from the Upper Cretaceous of Var, southern France", *Ann. Paléontol.* **108** (2022), article no. 102536.

Tortosa, T., *Vertébrés continentaux du Crétacé supérieur de Provence (Sud-Est de la France)*, PhD thesis, Université Paris 6: Paris (France), 2014. Online at https://theses.fr/2014PA066608 (accessed on September 26, 2025).

Tortosa, T., E. Buffetaut, N. Vialle, Y. Dutour, E. Turini and G. Cheylan, "A new abelisaurid dinosaur from the Late Cretaceous of southern France: palaeobiogeographical implications", *Ann. Paléontol.* **100** (2014), pp. 63–86.

Tortosa, T. and S. Leleu, "Les bassins continentaux et la première orogenèse provençale au Crétacé final : du Santonien terminal au Maastrichtien (−85 Ma à −66 Ma)", in *Géologie des Bouches-du-Rhône — Roches et paysages remarquables* (Bourrideys, J., ed.), Éditions BRGM: Orléans, 2021, pp. 87–104.

Tortosa, T. and M. Vianey-Liaud, "Éclosion d'une réserve", in *Les Cahiers de la Réserve Naturelle de Sainte-Victoire*, vol. 2, Éditions du Département des Bouches-du-Rhône: Marseille, 2021, p. 160. Online at https://hop-lesite.fr/ressources (accessed on November 1, 2025).

Tucker, R. T., K. E. Venter, C. Lana, E. M. Roberts, T. Chinzorig, K. Tsogtbaatar and L. E. Zanno, "U–Pb calcite age dating of fossil eggshell as an accurate deep time geochronometer", *Commun. Earth Environ.* **6** (2025), article no. 872.

Turin, G., "Description de deux espèces nouvelles du genre *Lychnus* (Mollusca, Gastropoda, Anadromidae) au Rognacien (Maastrichtien supérieur) de Vitrolles (Bouches-du-Rhône, France)", *Bull. Soc. Géol. Fr.* **188** (2017), article no. 38.

Valentin, X., P. Godefroit, R. Tabuce, M. Vianey-Liaud, W. Wenhao and G. Garcia, "First Late Maastrichtian (Latest Cretaceous) vertebrate assemblage from Provence (Vitrolles-la-Plaine, southern France)", in *Bernissart Dinosaurs and Early Cretaceous Terrestrial Ecosystems* (Godefroit, P., ed.), Indiana University Press: Bloomington, IN, 2012, pp. 583–597.

Vermeesch, P., "IsoplotR: a free and open toolbox for geochronology", *Geosci. Front.* **9** (2018), pp. 1479–1493.

Vianey-Liaud, M. and G. Garcia, "The interest of French Late Cretaceous dinosaur eggs and eggshell", in *First International Symposium on Dinosaur Eggs and Babies, Isona i Conca Della, Catalonia, Spain* (Bravo, A. M. and T. Reyes, eds.), 1999, pp. 165–176.

Vianey-Liaud, M., P. Mallan, O. Buscail and C. Montgelard, "Review of French dinosaurian eggshells: morphology, structure, mineral and organic composition", in *Dinosaur Eggs and Babies* (Carpenter, K., K. F. Hirsh and J. R. Horner, eds.), Cambridge University Press: Cambridge, 1994, pp. 151–183.

Vila, B., F. D. Jackson, J. Fortuny, A. G. Sellés and À. Galobart, "3-D Modelling of megaloolithid clutches: insights about nest construction and dinosaur behaviour", *PLoS One* **5** (2010), article no. e10362.

Woodhead, J. and J. Petrus, "Exploring the advantages and limitations of in situ U–Pb carbonate geochronology using speleothems", *GChron* **1** (2019), pp. 69–84.